METAL-TCPP DOPED UIO-66 WORKING AS PROMISING CATALYSTS FOR SULFIDES OXIDATION REACTION

A Thesis

by

YUTAO HUANG

Submitted to the Graduate and Professional School of
Texas A&M University
in partial fulfillment of the requirements for the degree of

MASTER OF SCIENCE

Chair of Committee,	Hongcai Zhou
Committee Members,	Marcetta Darensbourg
	Xin Yan
	Ya Wang
Head of Department,	Simon North

December 2021

Major Subject: Chemistry

ABSTRACT

Porphyrin and porphyrin derivatives are widely used in various applications due to their excellent photophysical and electrochemical properties. However, inherent defects (such as instability and self-quenching under physiological conditions) limit its application. To overcome these problems, various carriers have been developed to encapsulate, physically adsorb, or covalently bind porphyrin and porphyrin derivatives, such as micelles[1], liposomes[2], carbon nanotubes[3], inorganic nanoparticles[4], and polymer nanoparticles[5]. In recent years, the metal-organic framework (MOF) has received more and more attention. Introducing porphyrin molecules into MOF or using porphyrin as an organic linker to construct porphyrin-based MOF can combine the unique functions of porphyrin and MOF and overcome the limitations of porphyrins.[6] The loading of porphyrin in the MOF channel and the modification of porphyrin on the surface of MOF are effective strategies for the synthesis of porphyrin@MOF, enhancing the stability of porphyrin and promote potential applications. In this thesis, metal-TCPP(2,3,5,6-tetrakis(4-carboxyphenyl)pyrazine), a kind of porphyrin, was used to dope into a known MOF, UiO-66 to study the morphology and catalytic ability of the final product. Also, different BDCs(1,4-benzenedicarboxylate) are used to see the effect of different functional groups. Sulfide converting to sulfoxide and sulfones was chosen as the primary reaction we decided to study as the products are simple and easy to analyze using the NMR spectrum.

DEDICATION

To my beloved family and relatives for their support.

To all my friends who helped me with my life and study.

ACKNOWLEDGEMENTS

I would like to thank my committee chair, Dr.Zhou, and my committee members, Dr.Darensbourg, Dr.Yan, and Dr.Wang, for their instructions throughout the past two years.

Special thanks to Kunyu Wang and Dr. Liang Feng, my mentors and instructors at Texas A&M University. Thank you for offering suggestions in chemistry education. I am grateful for your contributions

Thanks to all of my friends and lab mates for encouraging and helping me in research and life in Texas A&M University.

My extended gratitude to all the department faculty and staff for making my life in Texas A&M University meaningful and wonderful.

Finally thanks to my parents for their long-lasting love and support all the time.

CONTRIBUTORS AND FUNDING SOURCES

Contributors

This work was supervised by a thesis committee consisting of Professor Hongcai Zhou, Marcetta Darensbourg, Xin Yan of the Department of Chemistry and Professor Ya Wang of the Department of Mechanical Engineering.

All work conducted for the thesis was completed by the student independently.

Funding Sources

Graduate study was supported by a fellowship from Texas A&M University.

NOMENCLATURE

MOF	Metal-Organic Frameworks
TCPP	2,3,5,6-tetrakis(4-carboxyphenyl)pyrazine
UiO	The University of Oslo
BA	Benzoic acid
PCN	Porous Coordination Network
NMR	Nuclear Magnetic Resonance
PXRD	Powder X-Ray Diffraction
DMF	N,N-Dimethylformide
BDC	1,4-benzenedicarboxylate
ICP-MS	Inductively coupled plasma mass spectrometry

TABLE OF CONTENTS

Page

LIST OF FIGURES

Page

LIST OF TABLES

1. INTRODUCTION

1.1. MOF synthesis and applications

A metal-organic framework (MOF)[7] classifies organic-inorganic hybrids constructed from metal-containing nodes and organic linkers. Metal-containing centers and organic bridging ligands can wisely select the topology, structure, pore environment, and function of MOF. Theoretically, the combinations of various joints and metals or metal clusters used to construct new MOFs are unlimited. Due to the characteristics of mixed composition, large surface area, adjustable pore size, adjustable function, and diversified structure, MOF has attracted significant attention and has been successfully applied in a wide range of research fields, such as gas adsorption[8, 9], luminescence[10], chemistry sensing[11], ion conduction[12], and heterogeneous catalysis[13]. Compared with traditional heterogeneous catalysts, the pore environment of MOFs can be well defined and fine-tuned to suit specific guest molecules. In addition, various organic and organometallic catalytic centers and nanoparticles can be directly synthesized or immobilized in MOF after synthesis to form well-defined active sites in a periodic and ordered structure. However, most MOFs are composed of soft acids (low oxidizing transition metal ions) and hard bases (carboxylates), so their chemical stability is relatively weak, dramatically limiting their application in heterogeneous catalysis. In order to improve the stability of MOF and gain insight into its catalytic activity, synthetic strategies must first be adopted to create a chemically stable MOF. We pay special attention to MOFs based on Zr polycarboxylates because of their high chemical stability and simple structure. Compared with MOF based on low-valent metal cations,

the strong Zr-O bond on the highly charged and oxophilic Zr(IV) cation explains this enhanced stability[14,15].

1.2. MOF doping techniques and types

It's not a novel idea to dope MOF with different compounds to modify the property of the MOF. Wenbin Lin's group[16] is interested in using MOF as a platform to integrate various functional components of solar energy collection. They report the development of the first MOF-based heterogeneous catalysis system for water oxidation, photocatalytic CO_2 reduction, and visible-light-driven organic photocatalysis. They doped the MOF with a metal complex.

MOFs can also be doped with nanoparticles. By combining the developed Ni and Pt-Ni alloys and performing corresponding calcinations, a new strategy for synthesizing highly active and robust ORR electrocatalysts has been proposed by Anand Parkash[17]. Because Ni and Pt-Ni nanoparticles have high catalytic activity in the N-doped carbon matrix, their porous structure can increase the visibility of active centers, accelerate intermediate migration, and have a larger specific surface area.

1.3. Previously reported examples of the effect of axial functional groups

In 2012, Cyrille Costentin[18] and his coworkers discussed the influence of local proton source (-OH) on the catalytic property of the Fe-TCPP. The trivalent metal centers in porphyrin rings usually come with an anion coordinated in the axial position, typically a Cl ion. Thus, the proton or other functional groups around will have strong interaction with the axial Cl, and the catalytic properties could be changed with different types of interactions. They found that the modification of iron tetraphenylporphyrin by

introducing phenolic groups at all the ortho and ortho positions of the phenyl group can significantly accelerate the catalysis of the reaction by the electro-generated iron (0) complex. The basis for the enhanced activity appears to be the high local proton concentration associated with the phenolic hydroxyl substituent.

The exact mechanism of phenol interference is currently unknown, but it is likely to be the same as the push-pull (electron-proton) type previously proposed for other acids. Regardless of the details of the mechanism, the enhanced catalytic activity of FeTDHPP is therefore related to a very high local phenolic proton concentration. We are considering whether other functional groups can produce similar results.

There is already a comparable model that is the metallocofactors in the enzyme pocket. In 2018, Ma[19] and his coworkers reported a unique strategy to develop an H_2O_2-dependent cytochrome P450BM3 system that catalyzes the mono-oxidation of synthetic substrates with the help of bifunctional small molecules (DFSM), such as N-(ω-imidazolyl fatty acyl)-l-amino acid. The acyl amino acid group of DFSM is responsible for binding to the enzyme as an anchor group, while the imidazole group acts as a general acid-base catalyst in the activation of H_2O_2. In the previously reported P450-H_2O_2 system, the system provides the best peroxidase activity for epoxidation of styrene, sulfonation, and oxidation of phenyl sulfide, and hydroxylation of ethylbenzene. This work provides the first example of the activation of P450, which is usually inert to H_2O_2, by introducing small exogenous molecules. This method improves the potential use of P450 in organic synthesis because it avoids the costly consumption of the reduced nicotinamide cofactor NAD(P)H and its dependent electron transport system. This

introduces a promising method based on direct chemical intervention in the catalysis process to utilize enzyme activity and function.

2. SYNTHESIS OF M-TCPP DOPED UIO-66

2.1. Introduction

UiO-66 doped with M-TCPP will be utilized as the first model. Here are the reasons. First, the pore size of UiO-66 is not too large, ensuring the mimicry of the enzyme pocket. Second, also the BDC linker for synthesizing UiO-66 can change to other BDC with functional groups. What's more, the distance between M-TCPP and functional BDCs is not too far. At the same time, the local chemical environments created by the functional BDCs could influence the behavior of M in the TCPP center.

UiO-66[20] is a typical Zr-MOF composed of Zr_6 clusters and 1,4-phthalate (BDC). The Zr_6 cluster is compatible with different types of organic joints due to its multifunctional symmetry and connectivity. UiO-66's high connectivity allows highly defective frameworks or sub-networks when reducing connectivity.

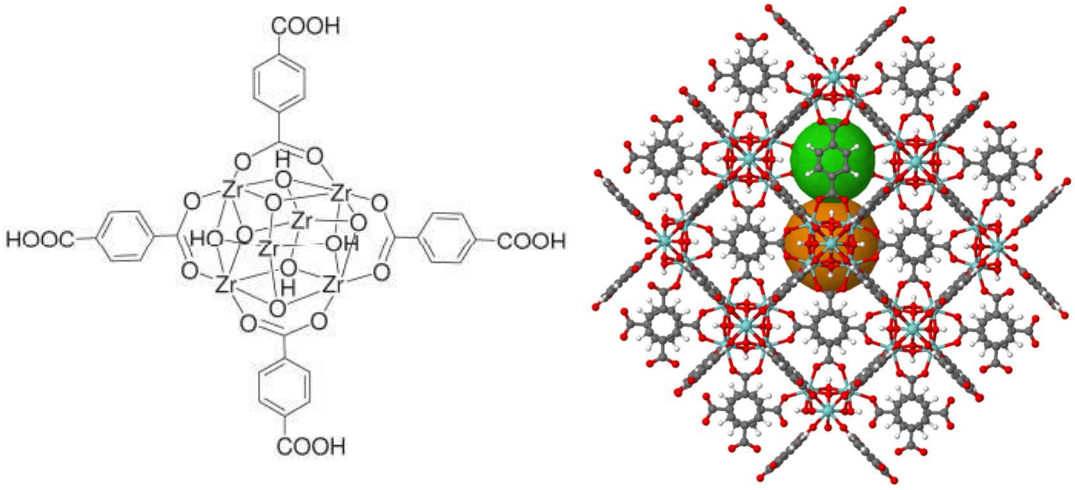

Figure 1. UiO-66 structure and 3D model

In addition, the available coordination sites on the Zr_6 cluster can reduce connectivity, which facilitates the combination of other functional parts. Therefore,

UiO-66 can tolerate different linkers with various topologies and functions. It is worth noting that compared with Zn/Cu/Cd-based MOF, UiO-66 shows significantly improved stability. It can still maintain good crystallinity under high external pressure and harsh chemical conditions.

Fixing TCPP on UiO-66 is of great value because TCPP can produce large-scale defects in the framework to improve adsorption and prevent catalytic deactivation or aggregation of porphyrins, thereby improving the performance of porphyrin catalysts.

Minghao Ni et.al[21] studied the structure of UiO-66-TCPP. The UV-vis absorption spectrum confirmed that TCPP was successfully encapsulated into the UiO-66 framework. For UiO-66, it can only be found that the absorption at the wavelength of 260 nm is the ring on the BDC ligand induced by benzene, and no prominent peak is observed from 300 nm to 700 nm. In contrast, the three spectra of TCPP-doped samples showed a strong characteristic peak with a wavelength of 423 nm and four weak peaks with a wavelength range of 500-700 nm, which belonged to the Soret band and Q band of the porphyrin ring.

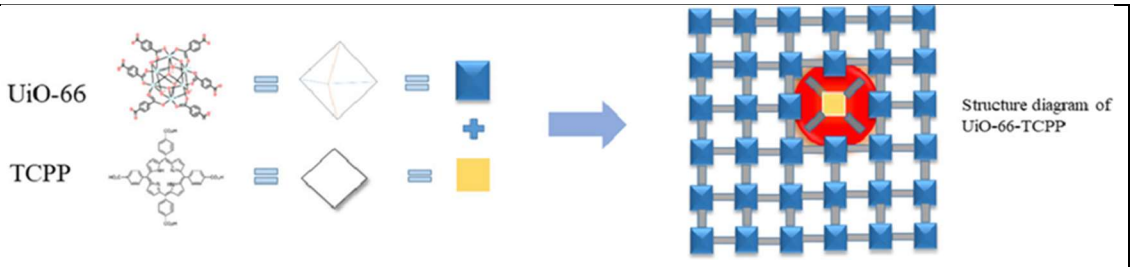

Figure 2. Structure of UiO-66-TCPP(Reprinted from Ref.[21])

6 BDCs were selected from the inventory, which includes 2-aminoterephthalic acid, monosodium 2-sulfoterephthalate, 2-bromoterephthalic acid, pyromellitic acid, 2-nitroterephthalic acid, and 2,5-dihydroxyterephthalic acid. Fe-TCPP and Mn-TCPP are

used to dope into UiO-66. Iron and manganese both have different oxidation states and can work as catalysts.

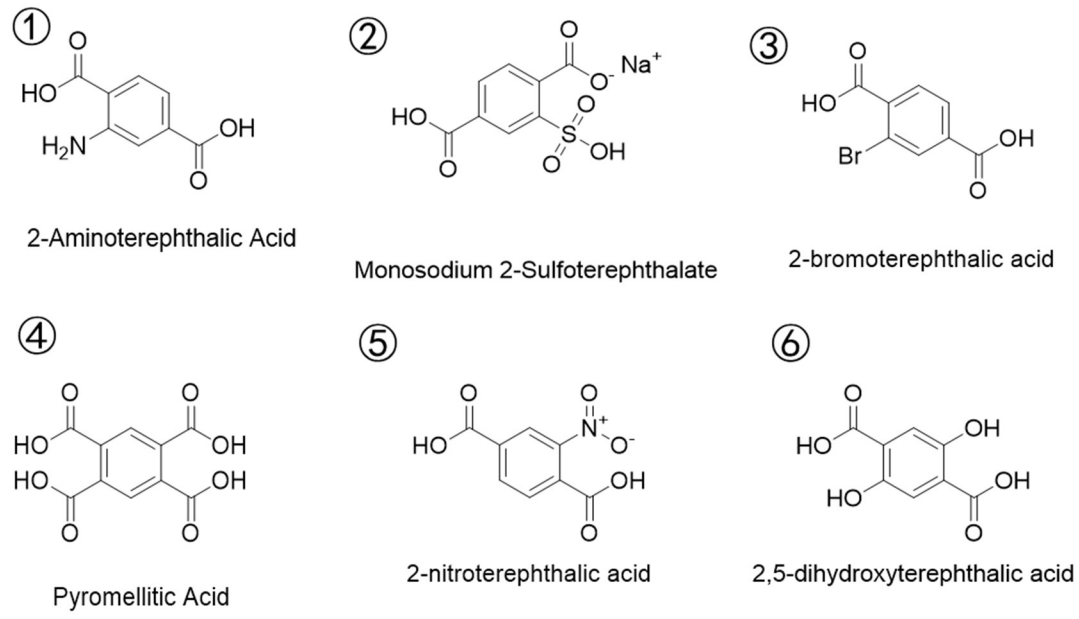

Figure 3. 6 BDCs used in this paper

2.2. Experiment part

2.2.1. Materials and Instrumentation

2.2.1.1. Materials

$ZrOCl_2 \cdot 8H_2O$, 2-aminoterephthalic acid, monosodium 2-sulfoterephthalate, 2-bromoterephthalic acid, pyromellitic acid, 2-nitroterephthalic acid, 2,5-dihydroxyterephthalic acid, BA(benzoic acid), DMF(N,N-Dimethylformamide), H_4TCPP(2,3,5,6-tetrakis(4-carboxyphenyl)pyrazine), DMA(N,N'-dimethylacetamide), FA(formic acid)

2.2.1.2. Instrumentation

PXRD(Powder X-ray diffraction) was carried out with Bruker D8-Focus Bragg-Brentano X-ray Powder Diffractometer equipped with a Cu sealed tube(λ=1.54178) at 40 kV and 40mA.

2.2.2. Procedure

2.2.2.1. Synthesis of UiO-66-NO_2-TCPP/ UiO-66-NH_2-TCPP/ UiO-66-Br-TCPP

UiO-66-TCPP-5% was synthesized based on the following procedure. $ZrOCl_2 \cdot 8H_2O$ (150 mg), H_2BDC (100 mg) and BA (2500 mg) dissolved in 10 mL N,N-Dimethylformamide (DMF) in a heat-resistant glass bottle. The vial was heated at 120 °C for 1 hour to obtain a clear, colorless solution, to which H_4TCPP (40 mg) was added. The vial was kept at 120 °C for one day. The solution was centrifuged, and the product in the form of a red powder was repeatedly washed with DMF.

2.2.2.2. Synthesis of UiO-66-$(OH)_2$-TCPP/ UiO-66-SO_3Na-TCPP/ UiO-66-$(COOH)_2$-TCPP

Different methods were used to synthesize these three MOFs because we found that they won't generate the expected products, and most of the products are PCN-224. So some slight modifications were made to the previously reported method.[22,23]

Dissolve $ZrOCl_2 \cdot 8H_2O$ (100 mg, 0.31 mmol), monosodium 2-sulfoterephthalate (83 mg, 0.31 mmol) and formic acid (1.17 mL, 31.03 mmol) in 3 mL of N,N'-dimethylacetamide (DMA). Put the mixture in a glass vial. The tube was sealed and heated to 120 °C and maintained at that temperature for 24 hours, and then cooled to room temperature. The precipitate was collected by filtration and dried in the air.

2.2.3. Mechanism

First, BA acts as a monocarboxylic acid regulator during the synthesis of MOF. Without the addition of TCPP or a small amount of TCPP, a competitive reaction will occur between BA and the ligand BDC, thereby regulating the rate of nucleation and crystal growth. In a DMF-based synthesis environment, the twelve edges of the Zr_6 cluster are occupied by twelve carboxylates from BDC. When a relatively large amount of TCPP is added to the system, the competition and coordination behavior will be transformed into a three-molecule system, including BA, BDC, and TCPP. However, the number of linked carboxylates from TCPP to Zr_6 clusters is variable (maybe six, eight, or twelve). Therefore, the above-mentioned unbalanced connection number will destroy the original periodic assembly of the metal and the ligand, resulting in a change in particle size.

2.3. Results and discussion

2.3.1. Photos

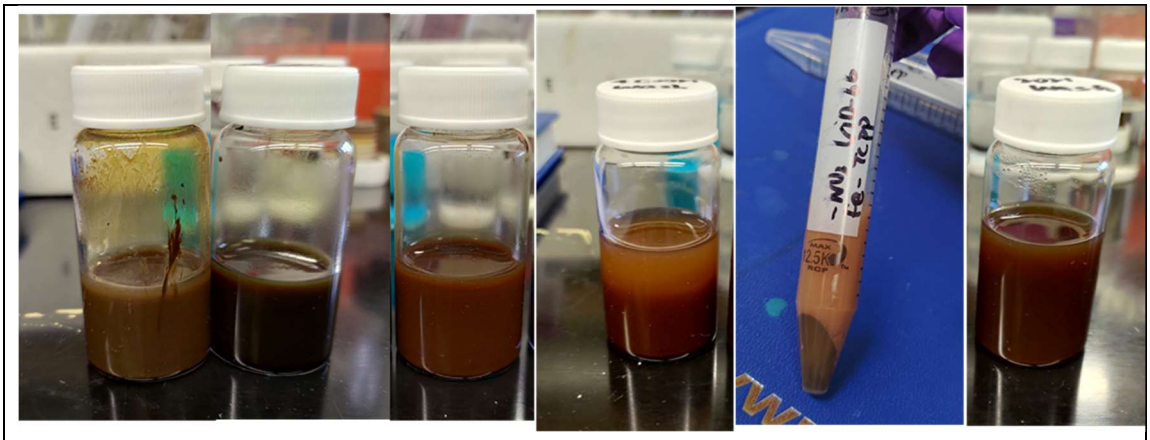

Figure 4. Graphs for Fe-TCPP doped UiO-66 with different functional groups

Figure 5. Graphs for Mn-TCPP doped UiO-66 with different functional groups

Generally, iron-TCPP doped UiO-66 display brown and dark brown color while manganese-TCPP doped UiO-66 display a color of green. Pure UiO-66 without TCPP will be white, and we can judge from the color to make a preliminary assertation that metal-TCPP was successfully incorporated into UiO-66.

2.3.2. Powder X-Ray Diffraction(PXRD)

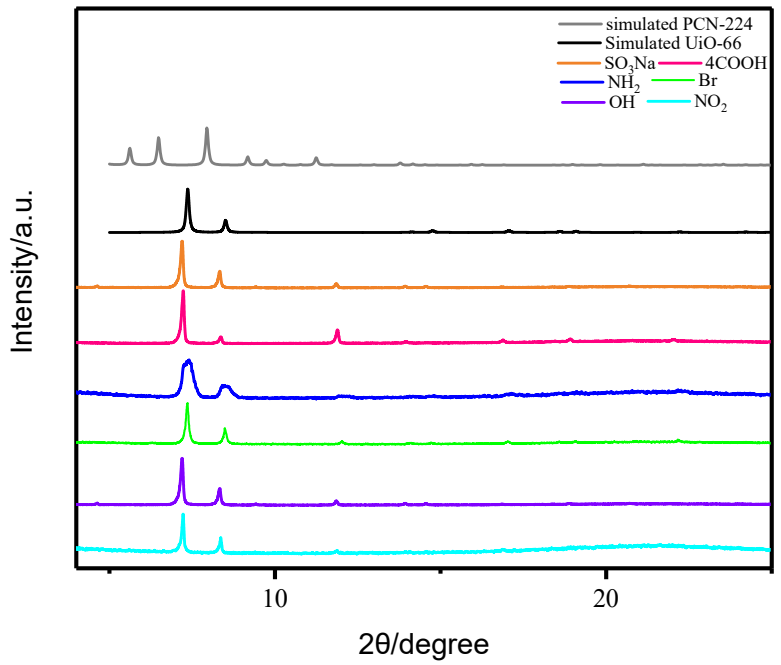

Figure 6. PXRD of Fe-TCPP doped UiO-66

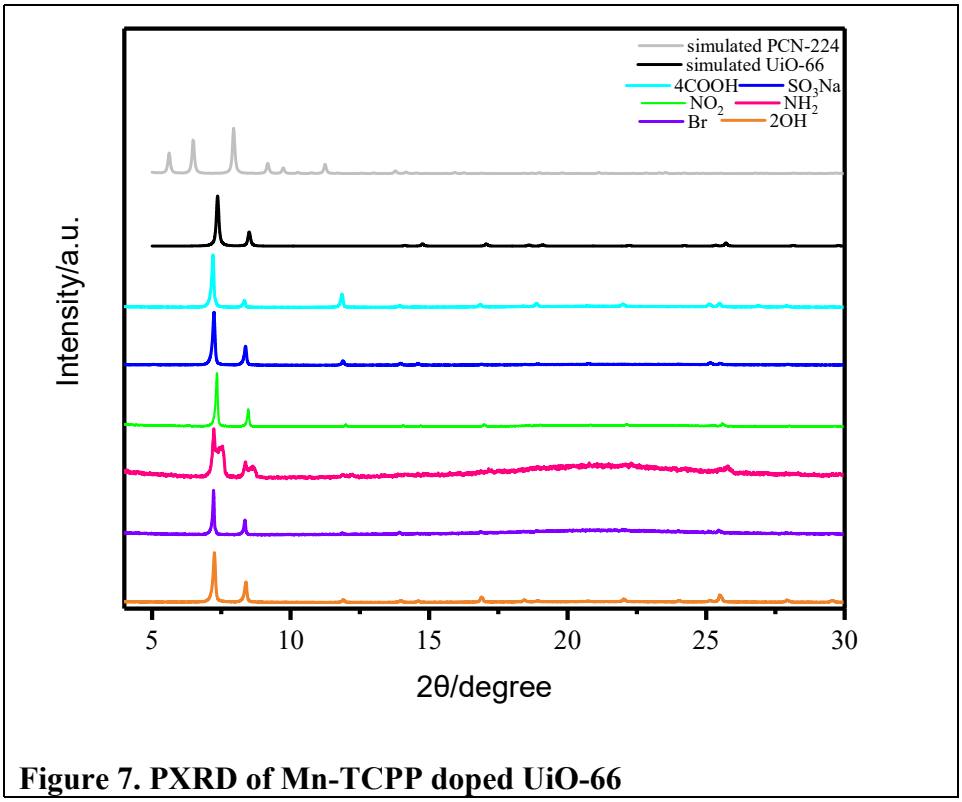

Figure 7. PXRD of Mn-TCPP doped UiO-66

From the PXRD pattern, we find that all the products are UiO-66 without any impurities that should be PCN-224. The typical peaks for UiO-66 are at 7 degrees and 8.5 degrees, while the ones for PCN-224 are at 5 degrees, 6 degrees and 8 degrees. We can find that all of our products have similar patterns to the simulated UiO-66 indicating their components. Metal-TCPP and different functional groups didn't have a significant effect on the PXRD pattern, which means the products still conserve the crystallinity of UiO-66.

2.3.3. Inductively coupled plasma mass spectrometry (ICP-MS)

Table 1.Molar ratio of UiO-66 and TCPP

Fe-TCPP	Molar ratio of Zr and Fe
UiO-66-NO_2	20:1

UiO-66-NH_2	**40:1**
UiO-66-Br	**36:1**
UiO-66-$(OH)_2$	**180:1**
UiO-66-$(COOH)_2$	**360:1**
UiO-66-SO_3Na	**75:1**

Table 2. Molar ratio of UiO-66 and Mn-TCPP

Mn-TCPP	Molar ratio of Zr and Mn
UiO-66-NO_2	**68:1**
UiO-66-NH_2	**94:1**
UiO-66-Br	**133:1**
UiO-66-$(OH)_2$	**750:1**
UiO-66-$(COOH)_2$	**1106:1**
UiO-66-SO_3Na	**383:1**

Several milligrams catalysts were dissolved using high concentrated nitric acid and heated under 80 Celsius overnight. Then the solution was diluted for ICP-MS running.

According to the ICP-MS results, we can find that iron incorporates more to UiO-66 than manganese. Among all functional groups, the metal-TCPP bind tightly to UiO-66 with nitro, amino, and Bromo groups than others. These results also confirm that metal-TCPP has been successfully doped into UiO-66. Later we can use this data to calculate the exact amount of catalytic components inside the MOF.

2.4. Summary

In this section, the metal-TCPP doped UiO-66 with different functional groups were successfully synthesized and different characterization methods were used to confirm its structure.

3. CATALYSIS REACTION STUDY USING M-TCPP DOPED UIO-66

3.1. Catalysis reaction introduction

Today, the negative effects caused by the presence of organic sulfur compounds in fuels have been fully confirmed. In addition to SO_X emissions from the combustion of organic sulfur compounds (usually related to the formation of acid rain), their presence is also a cause of catalyst poisoning and corrosion of internal combustion engines. Pires et al.[24] recently demonstrated the high efficiency of manganese (III) porphyrin and iron (III) porphyrin catalysts in oxidizing sulfur compounds by H_2O_2 under homogeneous conditions. Not only do they allow oxidative conversion without a co-catalyst, but they can also be effective if more environmentally friendly and sustainable protic solvents such as ethanol or methanol are used. Le Maux[25] and Simonneaux used chiral water-soluble iron porphyrin as a catalyst, successfully carried out the asymmetric oxidation of different sulfides through H_2O_2, and obtained optically active sulfoxides with an ee of up to 90%. Also, in 2011, it was reported that Fe(III) porphyrin was used to oxidize two sulfur compounds with oxygen directly.

The catalysts are MOFs containing porphyrin and iron or manganese, similar to the catalysts mentioned in the paper. So this reaction was tried to see their catalytic ability.

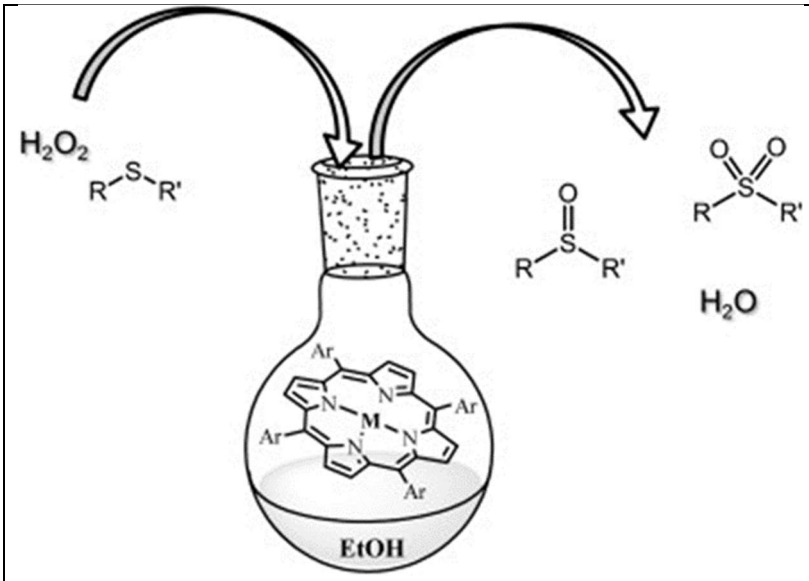

Figure 8. Catalysis reaction schema(Reprinted from Ref.[24])

3.2. Previously reported catalysts

In 2004, Baciocchi[26] reported that it only takes 4 minutes, 0.03%～0.09% catalyst, one equivalent of hydrogen peroxide, the separation rate for most sulfoxides can reach 90%-95%. When there is a cyano electron-withdrawing group on the benzene ring, a sulfoxide yield of 93% is still obtained. In addition, the reaction is not affected by steric effects, such as the yield of tert-butyl phenyl sulfoxide and diphenyl sulfoxide is 92%. No oxidation products were observed after the reaction for the substrate containing vinyl, alkene, propyl, hydroxyl, and other groups that are sensitive to oxidants. Adjust the amount of catalyst and hydrogen peroxide to 0.09% to 0.25%, two equivalents H_2O_2, react for 15 minutes, and sulfide can be quantified to sulfone by oxidation.

In 2011, Rajabi et al. [27]loaded iron oxide nanoparticles on SBA-15 and found that the catalyst can selectively oxidize sulfide to sulfoxide in a pure water medium, and the yield of the product is greater than 95%.

Using simple $FeCl_3$ and $FeBr_3$ as catalysts, Ren et al.[28] selectively oxidized diphenyl sulfide and methyl phenyl sulfide to sulfoxide at room temperature and in acetonitrile. Among them, the catalytic activity of $FeBr_3$ is stronger than that of $FeCl_3$.

Using chiral water-soluble iron porphyrin as a catalyst, asymmetric oxidation of sulfide by H_2O_2 in methanol and water to obtain optically active sulfoxide (ee up to 90%) was reported by Le Maux.[25]

3.3. Experiment Part

3.3.1. Materials and Instrumentation

3.3.1.1. Materials

Thioanisole, Ethanol(EtOH), Hydrogen peroxide(H_2O_2), the M-TCPP doped UiO-66 synthesized in chapter 2.

3.3.1.2. Instrumentation

Nuclear magnetic resonance(NMR) data were collected on a Mercury 300 spectrometer.

3.3.2. Experiment procedure

The substrate (0.3mmol) was dissolved in 2.0mL of ethanol and kept under magnetic stirring at 22-25℃ in the presence of the catalyst. The oxidant, diluted 1:10 in ethanol, was progressively added at regular intervals of 15 min in small aliquots, each corresponding to a half-substrate amount.

3.4. Results and discussion

3.4.1. Nuclear Magnetic Resonance Spectrum (NMR)

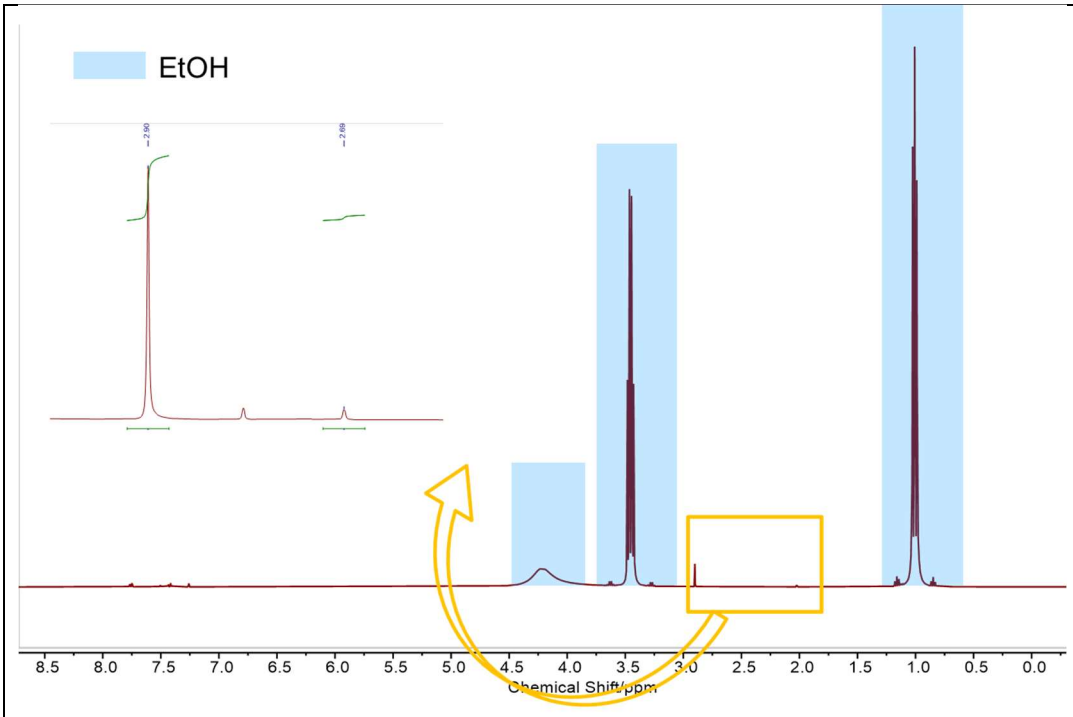

Figure 9. NMR spectrum for the mixture after the reaction

Searching from the NMR database, we got the spectrum for the starting material and the products.

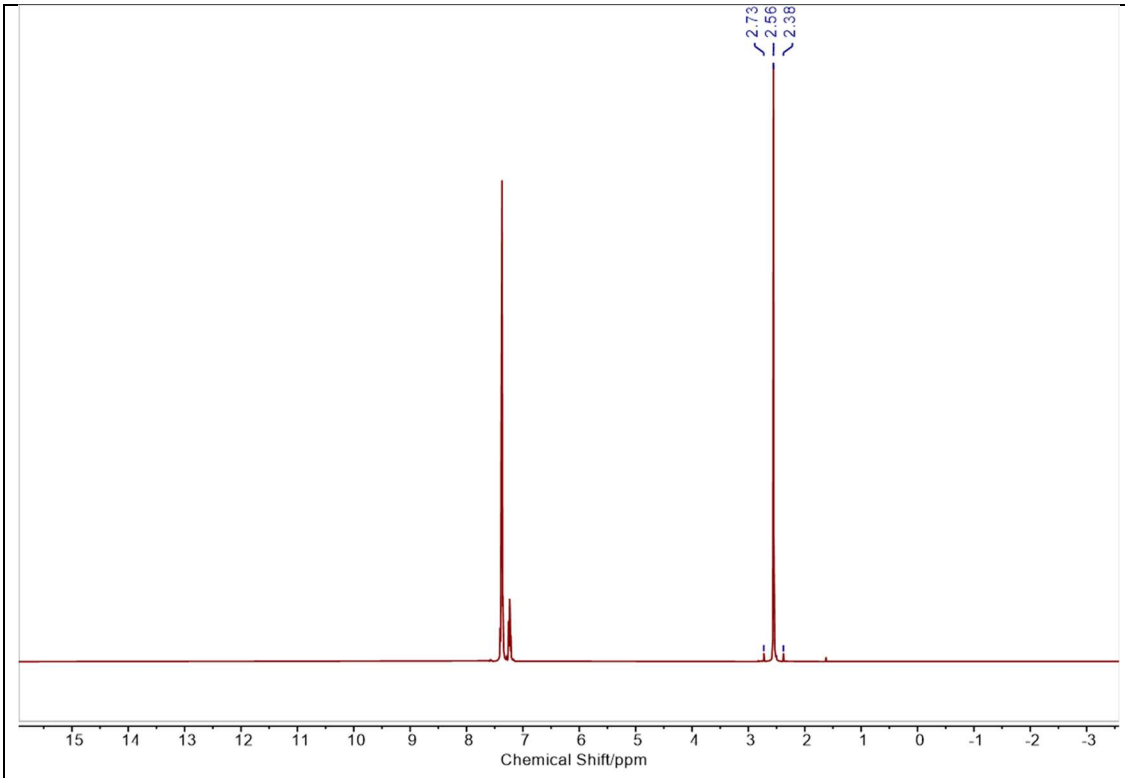

Figure 10. NMR spectrum for the sulfide

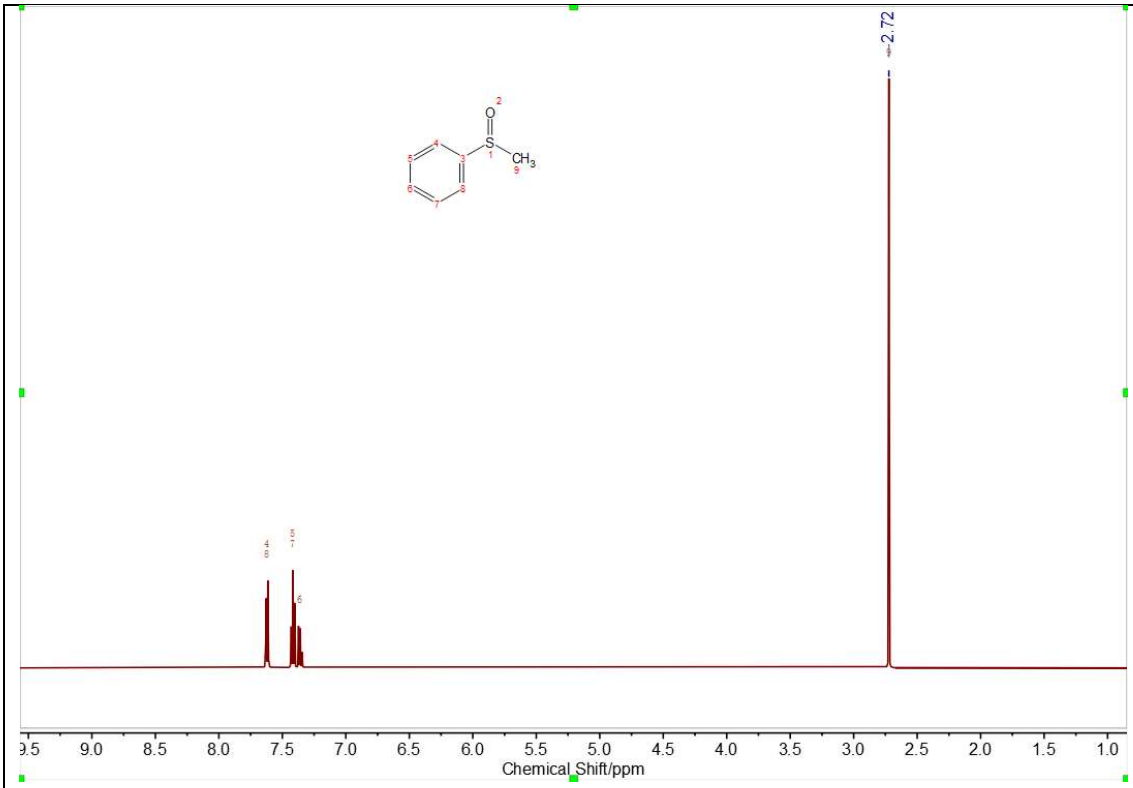

Figure 11.NMR spectrum for the sulfoxide

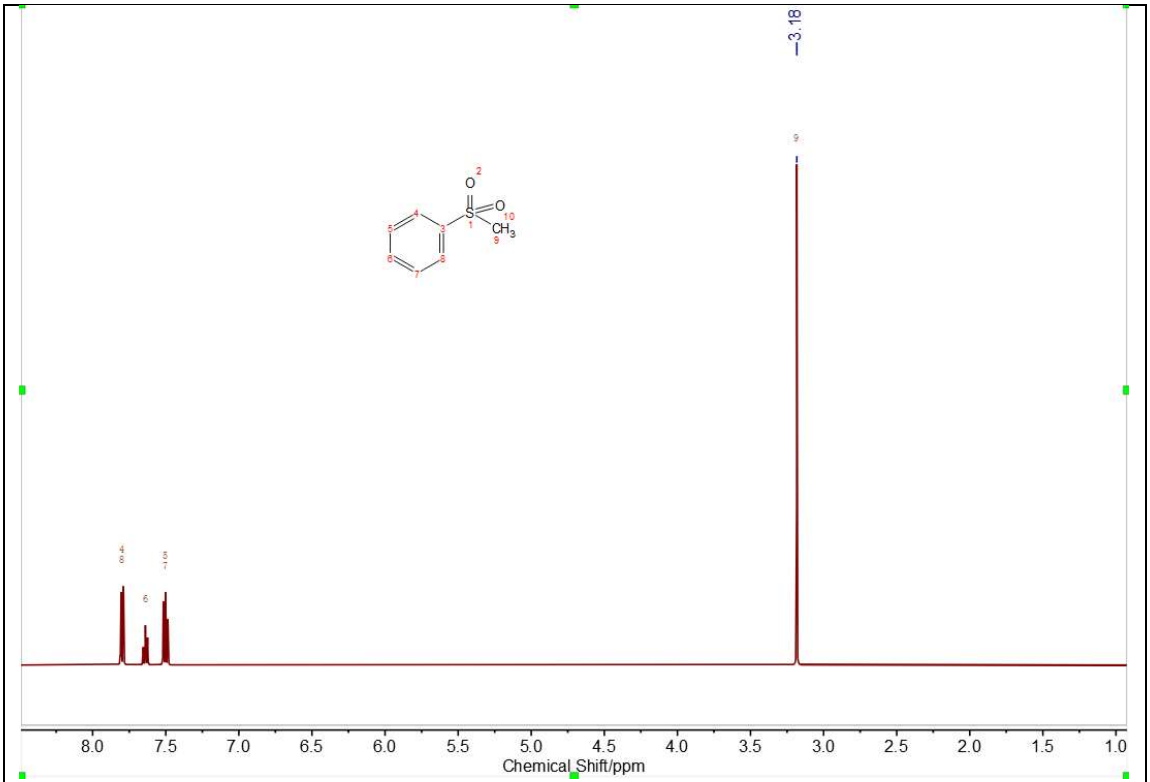

Figure 12. H-NMR spectrum for the sulfone

Table 3. Typical chemical shifts for all the reagents

reagent	Chemical shift
Starting material	2.56
sulfoxide	2.73
sulfone	3.18

We can find that all three have peaks between 2 and 3 and 7 and 8. However, the peaks between 7 and 8 are complicated and hard to analyze. So the singlet peak between 2 and 3 are chosen to calculate the ratio of the starting material and products.

3.4.2. Yield for different catalysts

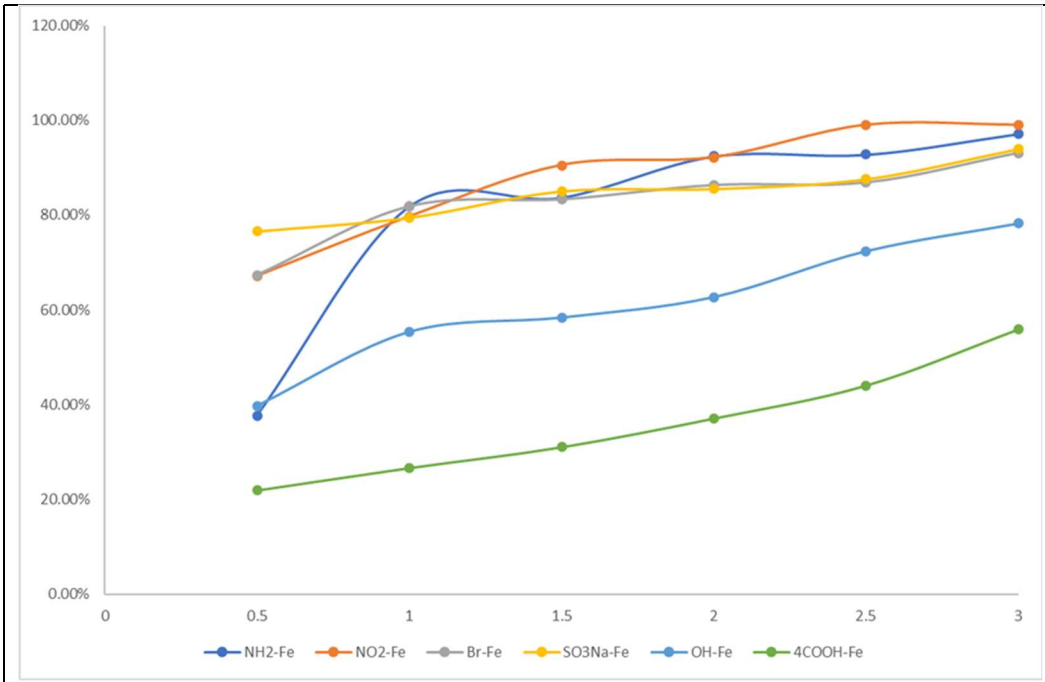

Figure 13. Yield change with time increasing for Fe-TCPP doped UiO-66 with different functional groups.

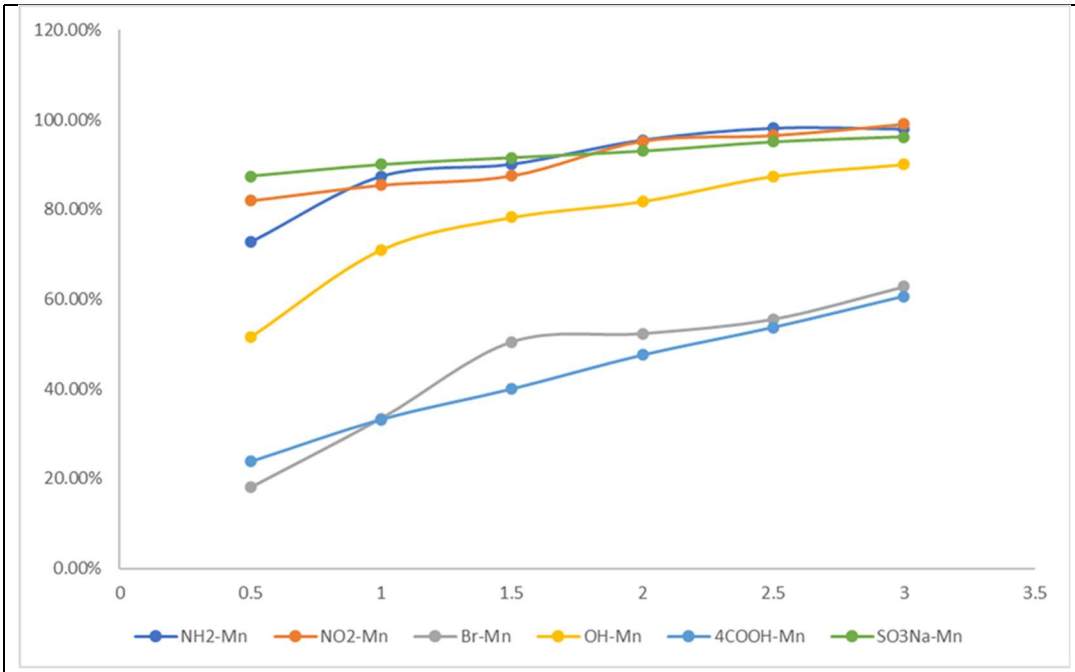

Figure 14. Yield change with time increasing for Mn-TCPP doped UiO-66 with different functional groups.

We can conclude from the yield-time graph that the yield increased until the reaction finished as time increased. Generally, most of the reaction will reach the end before 3 hours and get about 90% yield. However, as the amount of metal, which is the true catalyst inside the MOF is different, we need to introduce a new concept to describe the catalytic ability of the metal-TCPP doped UiO-66 quantitively.

3.4.3. TOF and comparison

Turnover Frequency (TOF) is a measure of the instantaneous efficiency of a catalyst. It is calculated as the derivative of the turnover of the catalytic cycle concerning the time of each active site. At such a low catalyst concentration, it exhibits infinite dilution behavior, and reactants and products (if possible) are saturated. [29]

$$TOF = Moles\ of\ products/(Time * Moles\ of\ catalysts)$$

We calculate the TOF at time= 0.5h, and the reason for that is at 0.5h, the reaction has not reached the end, and it's reliable to calculate the TOF. Later for some catalysts with excellent catalytic ability, the reaction may reach the end at some point, and the TOF calculated based on that will not be accurate.

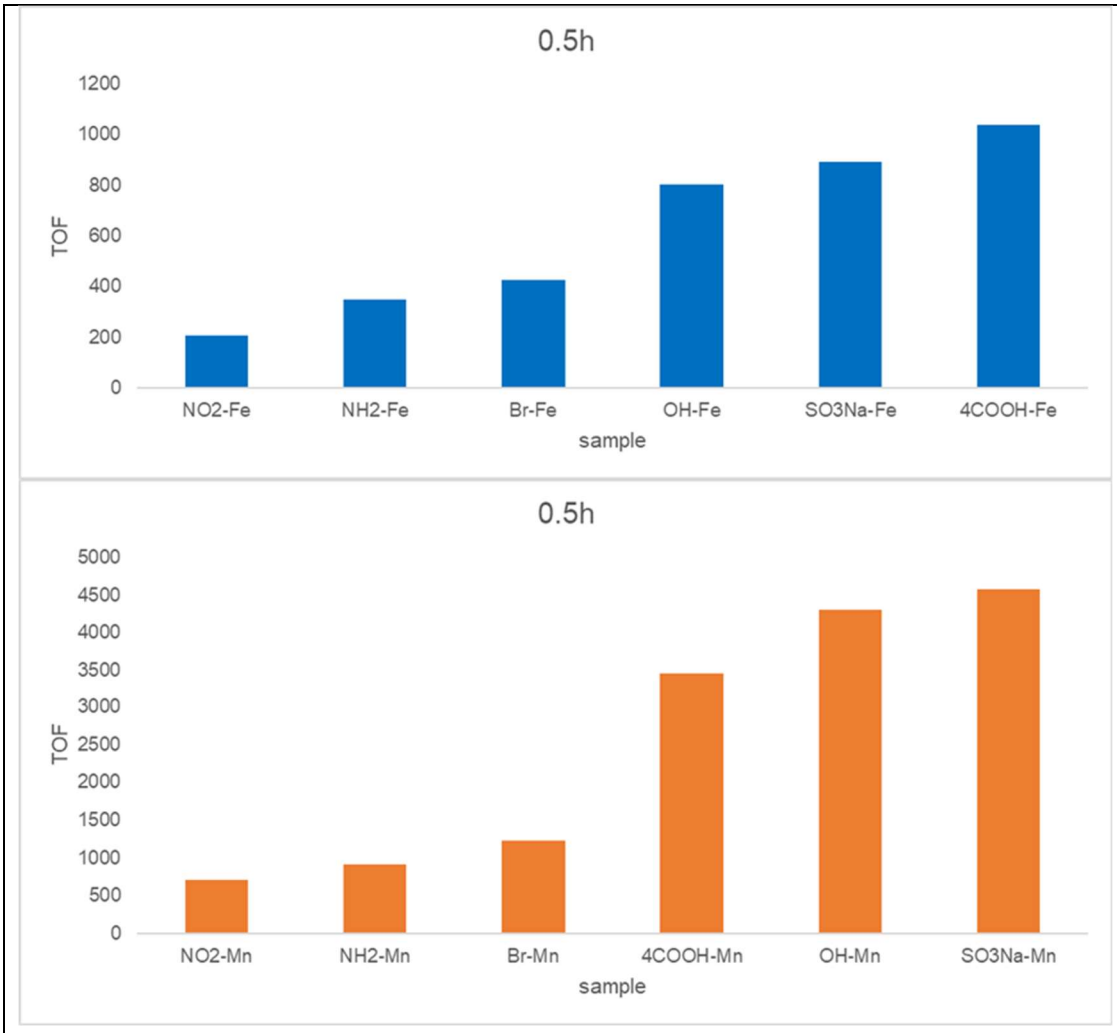

Figure 15. TOF for Fe-TCPP and Mn-TCPP doped UiO-66 with different functional groups at 0.5h

We can conclude that generally, for both Fe and Mn, the UiO-66 with 2OH, SO_3Na, and 4COOH have a larger TOF value than NO_2, NH_2 and Br.

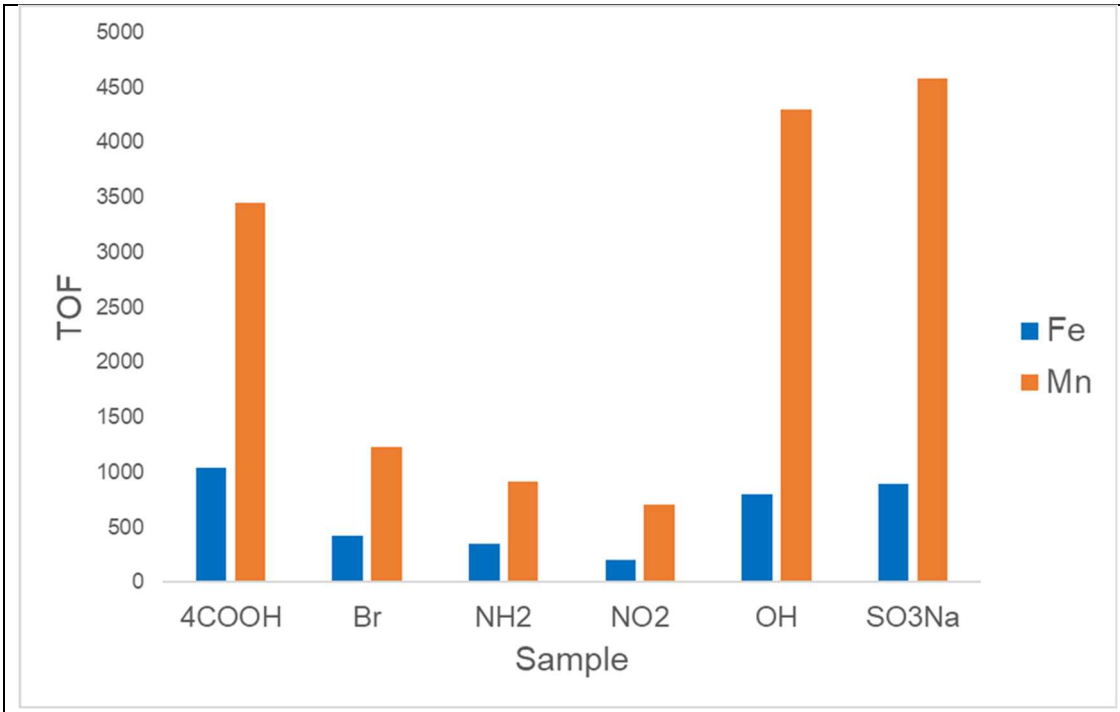

Figure 16. TOF comparison for Fe-TCPP and Mn-TCPP doped UiO-66

Besides, we also compare the TOF for Fe-TCPP and Mn-TCPP doped UiO-66 with different functional groups and find that manganese has a better catalytic ability than iron for all functional groups.

3.4.4. Control group

For control experiments, two groups were selected. One is the reaction without any catalysts, and another is the reaction using pure M-TCPP doped UiO-66 without additional functional groups.

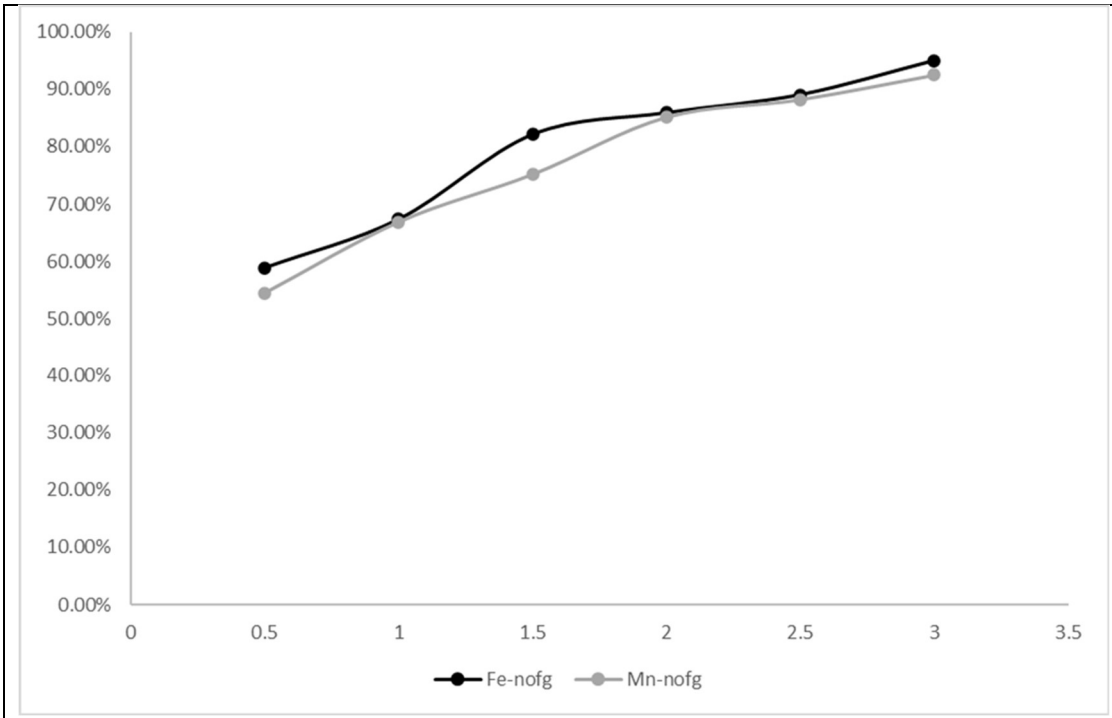

Figure 17. yield for the reaction using the metal-TCPP doped UiO-66 without any other functional groups.

We can find that, for the reaction without any catalysts, it will almost generate no products, which indicates the importance of catalysts. The reactions using the metal-TCPP doped UiO-66 without any other functional groups can generate some products. When comparing with those with different functional groups, we can assert that different functional groups generate different effects as some may accelerate the reaction and increase the yield while others may impede the reaction. This may be due to the electron-withdrawing and electron-pushing property of the functional groups.

4. CONCLUSIONS

This thesis has described the design and synthesis of metal-TCPP doped UiO-66 with different functional groups with various catalytic abilities and functionality.

In the first part, the employment of two different methods leads to producing a metal-TCPP doped UiO-66. This structure conserved the crystallinity of UiO-66, and the TCPP ligand was successfully incorporated into the framework rather than a simple physical mixture. ICP-MS technique clearly states the ratio of metal-TCPP and the UiO-66 framework, which provides detailed information for later calculation.

In the second part, one of the most common reactions that sulfide converted to sulfoxide and sulfones using hydrogen peroxide with the existence of catalysts was selected to study the catalytic ability of our metal-TCPP doped UiO-66. The yield change with time was recorded, and a concept TOF was introduced to describe our products' catalytic ability accurately. The NMR spectrum was used to analyze the ratio of starting material and final products.

By comparison, we concluded that our metal-TCPP doped UiO-66 has a relatively high catalytic ability in the sulfide converting to sulfoxides and sulfones reaction with a yield close to 90% and ee up to 90%. Generally, it is a very promising catalyst that can be used, and it brings a new method of doping ligand into known MOF to construct a new structure, turning the original catalytic inert MOF into an excellent catalyst.

REFERENCES

(1) Zhai, Y.; Busscher, H. J.; Liu, Y.; Zhang, Z.; van Kooten, T. G.; Su, L.; Zhang, Y.; Liu, J.; Liu, J.; An, Y.; Shi, L. Photoswitchable Micelles for the Control of Singlet-Oxygen Generation in Photodynamic Therapies. *Biomacromolecules* **2018**, *19* (6), 2023–2033. https://doi.org/10.1021/acs.biomac.8b00085.

(2) Wang, X.; Yan, F.; Liu, X.; Wang, P.; Shao, S.; Sun, Y.; Sheng, Z.; Liu, Q.; Lovell, J. F.; Zheng, H. Enhanced Drug Delivery Using Sonoactivatable Liposomes with Membrane-Embedded Porphyrins. *Journal of Controlled Release* **2018**, *286*, 358–368. https://doi.org/10.1016/j.jconrel.2018.07.048.

(3) Manickam, P.; Fernandez, R. E.; Umasankar, Y.; Gurusamy, M.; Arizaleta, F.; Urizar, G.; Bhansali, S. Salivary Cortisol Analysis Using Metalloporphyrins and Multi-Walled Carbon Nanotubes Nanocomposite Functionalized Electrodes. *Sensors and Actuators B: Chemical* **2018**, *274*, 47–53. https://doi.org/10.1016/j.snb.2018.07.133.

(4) Huang, P.; Qian, X.; Chen, Y.; Yu, L.; Lin, H.; Wang, L.; Zhu, Y.; Shi, J. Metalloporphyrin-Encapsulated Biodegradable Nanosystems for Highly Efficient Magnetic Resonance Imaging-Guided Sonodynamic Cancer Therapy. *J. Am. Chem. Soc.* **2017**, *139* (3), 1275–1284. https://doi.org/10.1021/jacs.6b11846.

(5) Cui, D.; Xie, W.; Zhang, S.; Liu, Z.; Liu, C.; Xu, Y. Copper Porphyrin-Based Conjugated Microporous Polymers as Photosensitizers for Singlet Oxygen Generation. *Materials Letters* **2018**, *232*, 18–21. https://doi.org/10.1016/j.matlet.2018.08.062.

(6) Chen, J.; Zhu, Y.; Kaskel, S. Porphyrin-Based Metal–Organic Frameworks for Biomedical Applications. *Angewandte Chemie International Edition n/a* (n/a). https://doi.org/10.1002/anie.201909880.

(7) Li, H.; Eddaoudi, M.; O'Keeffe, M.; Yaghi, O. M. Design and Synthesis of an Exceptionally Stable and Highly Porous Metal-Organic Framework. *Nature* **1999**, *402* (6759), 276–279. https://doi.org/10.1038/46248.

(8) Li, Y.; Yang, R. T. Gas Adsorption and Storage in Metal−Organic Framework MOF-177. *Langmuir* **2007**, *23* (26), 12937–12944. https://doi.org/10.1021/la702466d.

(9) Li, J.-R.; Kuppler, R. J.; Zhou, H.-C. Selective Gas Adsorption and Separation in Metal–Organic Frameworks. *Chem. Soc. Rev.* **2009**, *38* (5), 1477–1504. https://doi.org/10.1039/B802426J.

(10) Cui, Y.; Yue, Y.; Qian, G.; Chen, B. Luminescent Functional Metal–Organic Frameworks. *Chem. Rev.* **2012**, *112* (2), 1126–1162. https://doi.org/10.1021/cr200101d.

(11) Kreno, L. E.; Leong, K.; Farha, O. K.; Allendorf, M.; Van Duyne, R. P.; Hupp, J. T. Metal–Organic Framework Materials as Chemical Sensors. *Chem. Rev.* **2012**, *112* (2), 1105–1125. https://doi.org/10.1021/cr200324t.

(12) Li, X.; Zhang, H.; Wang, P.; Hou, J.; Lu, J.; Easton, C. D.; Zhang, X.; Hill, M. R.; Thornton, A. W.; Liu, J. Z.; Freeman, B. D.; Hill, A. J.; Jiang, L.; Wang, H. Fast and Selective Fluoride Ion Conduction in Sub-1-Nanometer Metal-Organic Framework Channels. *Nat Commun* **2019**, *10* (1), 2490. https://doi.org/10.1038/s41467-019-10420-9.

(13) Bavykina, A.; Kolobov, N.; Khan, I. S.; Bau, J. A.; Ramirez, A.; Gascon, J. Metal–Organic Frameworks in Heterogeneous Catalysis: Recent Progress, New Trends, and Future Perspectives. *Chem. Rev.* **2020**, *120* (16), 8468–8535. https://doi.org/10.1021/acs.chemrev.9b00685.

(14) Wang, S.; Wang, J.; Cheng, W.; Yang, X.; Zhang, Z.; Xu, Y.; Liu, H.; Wu, Y.; Fang, M. A Zr Metal–Organic Framework Based on Tetrakis(4-Carboxyphenyl) Silane and Factors Affecting the Hydrothermal Stability of Zr-MOFs. *Dalton Trans.* **2015**, *44* (17), 8049–8061. https://doi.org/10.1039/C5DT00421G.

(15) Mondloch, J. E.; Katz, M. J.; Planas, N.; Semrouni, D.; Gagliardi, L.; Hupp, J. T.; Farha, O. K. Are Zr6-Based MOFs Water Stable? Linker Hydrolysis vs. Capillary-Force-Driven Channel Collapse. *Chem. Commun.* **2014**, *50* (64), 8944–8946. https://doi.org/10.1039/C4CC02401J.

(16) Wang, C.; Xie, Z.; deKrafft, K. E.; Lin, W. Doping Metal–Organic Frameworks for Water Oxidation, Carbon Dioxide Reduction, and Organic Photocatalysis. *J. Am. Chem. Soc.* **2011**, *133* (34), 13445–13454. https://doi.org/10.1021/ja203564w.

(17) Parkash, A. Synthesis of Bimetal Doped Metal-Organic Framework (MOF-5): An Electrocatalyst with Low Noble Metal Content and High Electrochemical Activity. *ECS J. Solid State Sci. Technol.* **2020**, *9* (7), 075002. https://doi.org/10.1149/2162-8777/abade8.

(18) Costentin, C.; Drouet, S.; Robert, M.; Savéant, J.-M. A Local Proton Source Enhances CO2 Electroreduction to CO by a Molecular Fe Catalyst. *Science* **2012**, *338* (6103), 90–94. https://doi.org/10.1126/science.1224581.

(19) Ma, N.; Chen, Z.; Chen, J.; Chen, J.; Wang, C.; Zhou, H.; Yao, L.; Shoji, O.; Watanabe, Y.; Cong, Z. Dual-Functional Small Molecules for Generating an Efficient Cytochrome P450BM3 Peroxygenase. *Angewandte Chemie International Edition* **2018**, *57* (26), 7628–7633. https://doi.org/10.1002/anie.201801592.

(20) Valenzano, L.; Civalleri, B.; Chavan, S.; Bordiga, S.; Nilsen, M. H.; Jakobsen, S.; Lillerud, K. P.; Lamberti, C. Disclosing the Complex Structure of UiO-66 Metal Organic Framework: A Synergic Combination of Experiment and Theory. *Chem. Mater.* **2011**, *23* (7), 1700–1718. https://doi.org/10.1021/cm1022882.

(21) Ni, M.; Gong, M.; Li, X.; Gu, J.; Li, B.; Chen, Y. Dimensions of Fluorescence Kinetic Concentration of Doped Morphology Homologs Synthesized by TCPP and UiO-66 MOF. *Applied Materials Today* **2021**, *23*, 100982. https://doi.org/10.1016/j.apmt.2021.100982.

(22) Biswas, S.; Zhang, J.; Li, Z.; Liu, Y.-Y.; Grzywa, M.; Sun, L.; Volkmer, D.; Voort, P. V. D. Enhanced Selectivity of CO2 over CH4 in Sulphonate-, Carboxylate- and Iodo-Functionalized UiO-66 Frameworks. *Dalton Trans.* **2013**, *42* (13), 4730–4737. https://doi.org/10.1039/C3DT32288B.

(23) Biswas, S.; Voort, P. V. D. A General Strategy for the Synthesis of Functionalised UiO-66 Frameworks: Characterisation, Stability and CO2 Adsorption Properties. *European Journal of Inorganic Chemistry* **2013**, *2013* (12), 2154–2160. https://doi.org/10.1002/ejic.201201228.

(24) Pires, S. M. G.; Simões, M. M. Q.; Santos, I. C. M. S.; Rebelo, S. L. H.; Paz, F. A. A.; Neves, M. G. P. M. S.; Cavaleiro, J. A. S. Oxidation of Organosulfur Compounds

Using an Iron(III) Porphyrin Complex: An Environmentally Safe and Efficient Approach. *Applied Catalysis B: Environmental* **2014**, *160–161*, 80–88. https://doi.org/10.1016/j.apcatb.2014.05.003.

(25) Maux, P. L.; Simonneaux, G. First Enantioselective Iron- Porphyrin -Catalyzed Sulfide Oxidation with Aqueous Hydrogen Peroxide. *Chemical Communications* **2011**, *47* (24), 6957–6959. https://doi.org/10.1039/C1CC11675D.

(26) Baciocchi, E.; Gerini, M. F.; Lapi, A. Synthesis of Sulfoxides by the Hydrogen Peroxide Induced Oxidation of Sulfides Catalyzed by Iron Tetrakis(Pentafluorophenyl)Porphyrin: Scope and Chemoselectivity. *J. Org. Chem.* **2004**, *69* (10), 3586–3589. https://doi.org/10.1021/jo049879h.

(27) Rajabi, F.; Naserian, S.; Primo, A.; Luque, R. Efficient and Highly Selective Aqueous Oxidation of Sulfides to Sulfoxides at Room Temperature Catalysed by Supported Iron Oxide Nanoparticles on SBA-15. *Advanced Synthesis & Catalysis* **2011**, *353* (11–12), 2060–2066. https://doi.org/10.1002/adsc.201100149.

(28) Villalobos, L.; Ren, T. Oxygenation of Organic Sulfides Catalyzed by Simple Fe(III) Salts. *Inorganic Chemistry Communications* **2013**, *28*, 52–54. https://doi.org/10.1016/j.inoche.2012.11.010.

(29) Kozuch, S.; Martin, J. M. L. "Turning Over" Definitions in Catalytic Cycles. *ACS Catal.* **2012**, *2* (12), 2787–2794. https://doi.org/10.1021/cs3005264.